Dyes and Pigments 92 (2011) 531–536

Contents lists available at ScienceDirect

Dyes and Pigments

journal homepage: www.elsevier.com/locate/dyepig

Electronic structure and spectral properties of the triarylamine-dithienosilole dyes for efficient organic solar cells

Boris F. Minaev [a,b], Gleb V. Baryshnikov [a,*], Valentina A. Minaeva [a]

[a] Bohdan Khmelnytskyy National University, 18031 Cherkasy, Ukraine
[b] Theoretical Chemistry, School of Biotechnology, Royal Institute of Technology, SE-10691 Stockholm, Sweden

ARTICLE INFO

Article history:
Received 25 February 2011
Received in revised form
5 June 2011
Accepted 7 June 2011
Available online 21 June 2011

Keywords:
Triarylamine-dithienosilole dyes
Density functional theory
Bader analysis
Cremer–Kraka energy density
Electric dipole transition moment
Hydrogen bond

ABSTRACT

The recently synthesized high-performance triarylamine dyes with the dithienosilole π-conjugated spacer for efficient organic solar cells are calculated at the density functional theory (DFT) level with the Bader approach for the quantum theory of atoms in molecule (QTAIM) analysis. The presence of stabilizing intramolecular hydrogen bonds and Van der Waals interactions in the dye molecules is predicted and the energies of these interactions are estimated. The electronic bands nature in absorption spectra of the dyes is determined by the time-dependent DFT calculations with a linear response methodology using B3LYP and BMK hybrid functionals. Relations between incident light absorption intensity in the first long-wavelength band of the dye, its polarization, HOMO–LUMO orbital nature and the driving force of electron injection to the semiconductor are discussed.

1. Introduction

Triarylamine-dithienosilole dyes [1,2] represent a new class of sensitizing dyes for the high efficient solar cells of Grätzel type [3]. Some recently synthesized representatives of this class of dyes are the 2-cyano-3-{5′-{2-{4-[*N*,*N*-bis(4-(2-ethylhexyloxy)-phenyl)amino]phenyl}-3,4-ethylenedioxythiophene-5-yl}-3,3′-di-*n*-hexylsilylene-2,2′-bithiophene-5-yl}acrylic acid [1] (C219, Fig. 1a) and the 3-[5[*N*,*N*-bis(phenylamino)phenyl]-3,3′-diphenylsilylene-2,2′-bithiophene-5′-yl]-2-cyanoacrylic acid [2] (TPCADTS, Fig. 1b)

The TPCADTS and C219 dyes are typical supramolecular structures constructed by the donor–bridge–acceptor type (called the D–π–A structure). The diphenyl-dithienosilole (DD) group is used as a bridge in the TPCADTS dye and in the C219 dye the di-*n*-hexyl-dithienosilole (DHD) group is used, which is conjugated with ethylenedioxythiophene (EDOT) moiety. The usage of such bridging groups allows to obtain the high charge separation upon photoexcitation, which provides the better efficiency of the incident photon–electric conversion (IPEC), and therefore – the high efficiency of solar cells. Efficiency of solar cell, based on the TPCADTS dye is about 7% [2] and the efficiency of the devices, sensitized by the C219 dye is about 10–10.3% [1] under the standard global air mass 1.5 (AM 1.5G); this is an absolute record for organic solar cells (without use of the Ru-based dyes). The previous record belongs to the indoline dye D205 [4], which gives the efficiency of solar cells at the level of 9.52%. An important role in the efficiency increase of the solar cells is determined by two phenyl substituents in the DD group in the TPCADTS dye. In the C219 dye this role can be attributed to the bulky alkyl substituents (in DHD and in the triarylamine groups). They perform the role of "molecular dielectrics" and prevent recombination between electrons from the conduction band of the semiconductor with the redox pairs of the electrolyte, which occupy the inner space of the solar cell.

The spectral properties of these dyes have been proper studied by experimental methods of UV–visible and IR spectroscopy. However, a number of questions on the electronic structure of these molecules and the nature of their electronic absorption spectra remain far from being fully described in the literature. In this connection we have performed quantum-chemical calculations of the electronic structure and spectral properties of the investigated dyes.

2. Computational details

The structures of the TPCADTS and C219 dyes were optimized at the B3LYP/6-31G(d) [5–7] level of DFT using GAUSSIAN 03 package [8]. With the same method the IR spectra were calculated by the

* Corresponding author. Tel.: +38 0 472 322967; fax: +38 0 472 354463.
E-mail address: glebchem@rambler.ru (G.V. Baryshnikov).

0143-7208/$ – see front matter © 2011 Elsevier Ltd. All rights reserved.
doi:10.1016/j.dyepig.2011.06.012

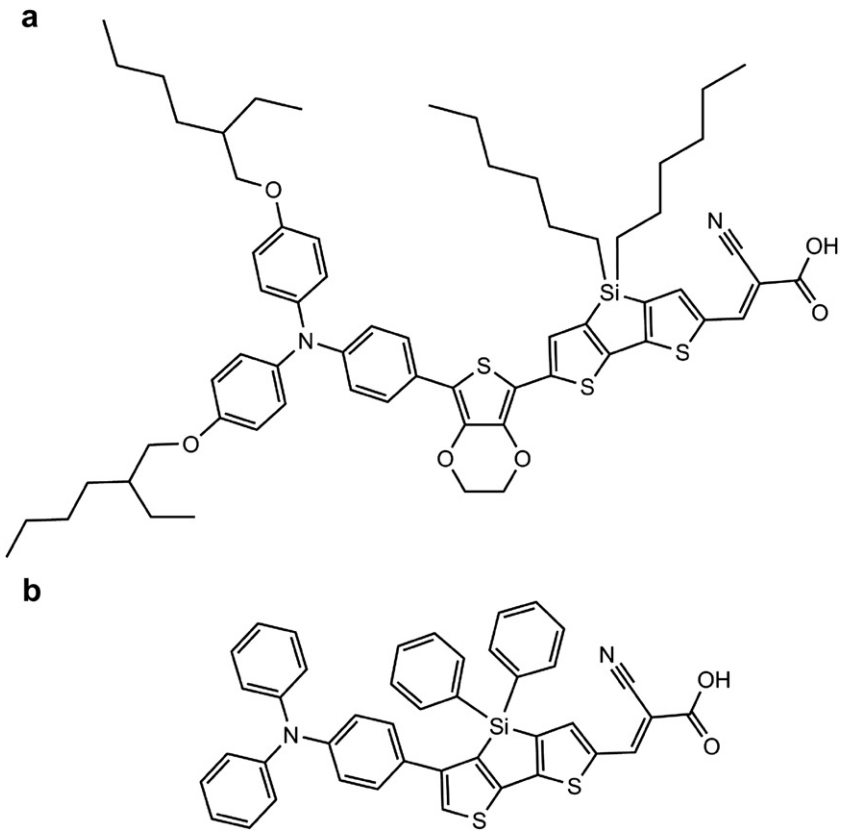

Fig. 1. Molecular structures of the C219 (a) and TPCADTS (b) dyes.

gradient approach to determine the true minimum of the total energy and vibrational frequencies. All vibrational mode frequencies are real, which indicates the true minimum of the total energy location. The molecular orbitals (MO) of the dyes were mapped from the single point energy calculation (iso-density surface values are fixed at 0.03 a.u.). While the B3LYP density functional is well known for its strong performance and reliability of the calculated molecular structures [5,9,10], its weakness to deal with the non-covalent interactions should be mentioned. There is also a concern that B3LYP functional is not well suited to treat charge separation states. Charge-transfer (CT) excited states are obtained in the studied dyes, thus we used also other functionals. The electronic excited state properties of the investigated dyes were calculated by the TD DFT method [9,10] using B3LYP and BMK (Boese-Martin for Kinetics [11]) hybrid functionals with the same 6-31G(d) basis set. The BMK method is parametrized for transition state treatment including redox processes, thus we believe it fits better for CT state calculation. The solvent effect on the electronic absorption spectra was taken into account using the polarized-continuum model (PCM) [12] with the acetonitrile as a model solvent. Fitting the electronic absorption spectra curves of the dye molecules was performed using the Gauss distribution function and a half-width of 3500 cm^{-1} with the SWizard 4.6. program package [13].

For the equilibrium geometry calculated by the B3LYP/6-31G(d) method we also analyzed the electron density distribution function $\rho(r)$ by the Bader method of quantum theory "Atoms in molecules" (QTAIM) [14]. Energy of intramolecular non-valence contacts in the dyes molecules are calculated by the formula of Espinosa [15,16].

$$E = 313.754 \cdot V(r) \quad (1)$$

where E is the energy of interatomic interaction (kcal/mol), $V(r)$ – potential energy density (a.u.) in the corresponding critical point (3, −1) [14]. According to Bader method, the critical point (3, −1) corresponds to the inflection of the electron density distribution function, that is an "indicator" of the chemical bond presence. Implementation of QTAIM method allows to describe chemical bonding at the qualitative level based on the characters of the Laplacian of electron density ($\nabla^2\rho$) in the critical point and the Cremer–Kraka energy density $H(r)$[17–19]:

1) $\nabla^2\rho < 0$, $H(r) < 0$ – weakly polar covalent bonds;
2) $\nabla^2\rho > 0$, $H(r) < 0$ – polar covalent bonds, strong hydrogen bonds;
3) $\nabla^2\rho > 0$, $H(r) > 0$ – interaction between closed-shells: hydrogen bonds and Van der Waals interaction.

The Cremer–Kraka energy density $H(r)$ is equal to the sum of potential energy density $V(r)$ value and kinetic energy density value in Lagrangian form $G(r)$:

$$H(r) = G(r) + V(r)$$

There is also a direct correlation between the Laplacian of the electron density and $V(r)$ and $G(r)$ values [14]:

$$\frac{1}{4}\nabla^2\rho = 2G(r) + V(r)$$

Equation (1) is valid for all types of hydrogen bonds, Van der Waals interactions and weak contacts such as H–H and CH–O interactions (second and third conditions).

Topological analysis of the electron density distribution function $\rho(r)$ by the QTAIM method was made using the AIMQB program, which is implemented in the AIMAll package [20]. All DFT calculations were performed on a PDC supercomputer at the KTH (Stockholm).

3. Results and discussion

3.1. Electronic structure and Bader analysis of $\rho(r)$ function

Calculation of the equilibrium geometry of the C219 dye (Fig. 2a) reveals that the EDOT, DHD and cyanoacrylic acid groups are situated in the same plane. This is due to the presence of stabilizing intramolecular O(1)–H(2), S(3)–O(4) and O(5)–H(6) bonds (Table 1, Fig. 2a). The O(1)–H(2) and O(5)–H(6) contacts represent the weak hydrogen bond interactions. The S(3)–O(4) contact is a closed-shell Van der Waals interaction. The total stabilization energy of these contacts in the stable C219 dye molecule conformation estimated by Eq. (1) is equal to 7.81 kcal/mol.

The cyanoacrylic acid fragment and DD group are also situated in the same plane. Their relative position is stabilized by the weak O(1)–H(2) hydrogen bond (Table 1, Fig. 2b).

Using the characters of the Laplacian of the electron energy density and the Cremer–Kraka energy density ($\nabla^2\rho > 0$, $H(r) > 0$) at the critical points we have found that all intramolecular bonds correspond to electronic interactions of the closed-shells, i.e. density is concentrated in the atomic space. This is also confirmed by the low value of electron density $\rho(r)$ (Table 1) in the corresponding critical points.

3.2. Electronic absorption spectra

Comparison of results obtained by the TD DFT–B3LYP method with the experimental data indicates that they are considerably different. For this reason, we have calculated excitation energies by exchange–correlation BMK functional, whose results have demonstrated the better agreement with experimental data than the B3LYP (Table 2). The Ref. [21] indicates that the B3 exchange functional yields a large error in calculating the triphenilamine–rhodanine dye exited states compared to experiment and other exchange functionals. Regarding the difference between the calculated and the experimental absorption spectra, it matters considerably less if the difference is consistent for all bands and compounds in order to make qualitative assignments. Indeed, the Table 2 indicates that all calculated vertical electronic transitions have similar assignments and almost consistent energy shifts between methods and compounds. In a consistent manner the B3LYP–TD DFT method strongly overestimates the absorption wavelengths in gas phase (and even more – in solvent). The BMK functional provides much better agreement with experiment (Table 2). Therefore we will describe the optical properties based on the BMK functional (Table 2, Fig. 3). Even in this case the charge-transfer states (visible band wavelengths) are overestimated for the long-bridge (C219) molecule. Such long-distance charge-transfer transition is a great challenge for any functionals. Involvement of non-covalent interactions in the C219 molecule (Fig. 2) provides additional problems for charge-transfer state description.

The absorption spectrum of the C219 dye calculated with the PCM solvent model (Fig. 3) shows two bands; the first one (short-wavelength) in the near UV–visible region of 350–470 nm (350–430 nm for TPCADTS) peakes at 377 (386) nm (experimental data are: 387 nm for C219 and 336 nm for TPCADTS) and the second one (long-wavelength visible) in the region of 470–700 nm (430–650 nm for TPCADTS) peakes at 571 (521) nm (experimental data are: 493 nm in for C219 and 495 nm for TPCADTS). The peak at 571 (521) nm is caused by a singlet–singlet π–π^* transition, which corresponds to the single-electron excitation from the highest occupied MO (HOMO) to the lowest unoccupied (LUMO), Fig. 4. Similar frontier orbitals have been obtained in Refs. [1,2], presented with a larger iso-density surface value (0.04). This transition is accompanied by charge-transfer from triphenilamine donor fragment to the cyanoacrylic-acid acceptor group through the DHD and

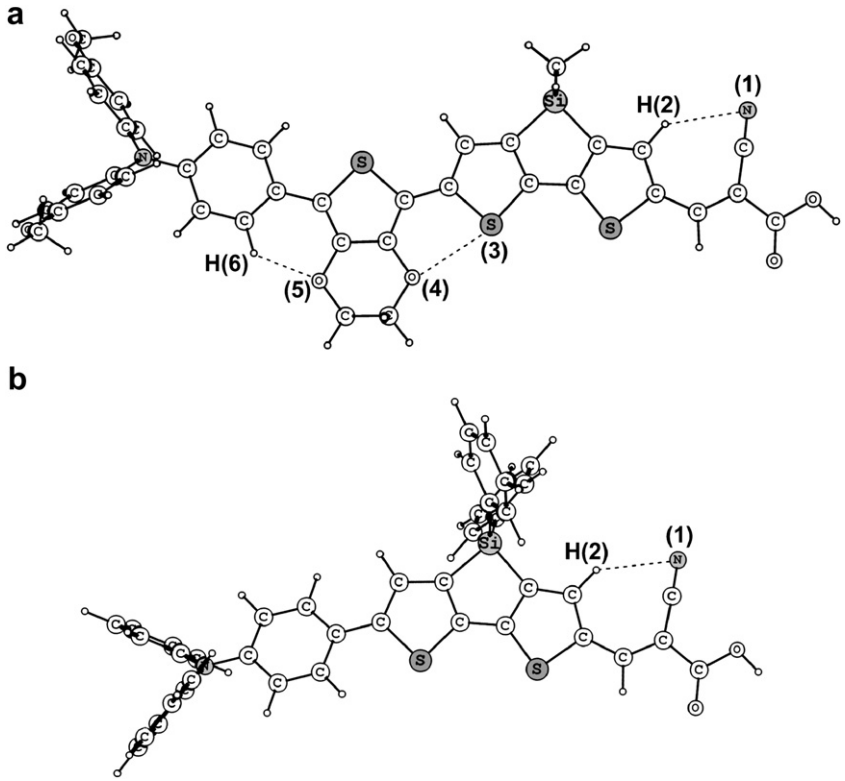

Fig. 2. Optimized configuration structures of the TPCADTS (b) and C219 (a) dyes. 2-Ethylhexyl and *n*-hexyl substituents are replaced by methyl groups.

Table 1
Parameters of non-valent interactions in the TPCADTS and C219 dyes.

Dye	Bond	$\rho(r)$, $e \times a_0^{-3}$ [a]	$V(r)$, *a.u.*	$G(r)$, *a.u.*	$H(r)$, *a.u.*	$\nabla^2\rho$, $e \times a_0^{-5}$	E, kcal/mol
TPCADTS	O(1)–H(2)	1.01×10^{-2}	-5.41×10^{-3}	7.29×10^{-3}	1.88×10^{-3}	3.67×10^{-2}	−1.70
C219	O(1)–H(2)	1.03×10^{-2}	-5.53×10^{-3}	7.41×10^{-3}	1.88×10^{-3}	3.72×10^{-2}	−1.74
	S(3)–O(4)	1.23×10^{-2}	-9.25×10^{-3}	9.99×10^{-3}	7.40×10^{-3}	4.29×10^{-2}	−2.90
	O(5)–H(6)	1.34×10^{-2}	-1.01×10^{-3}	1.13×10^{-3}	1.20×10^{-3}	4.97×10^{-2}	−3.17

[a] a_0 – Bohr radius (0.529 Å).

Table 2
Absorption properties of C219 and TPCADTS (parameters in parenthesis corresponds to gas phase calculations).

PCM/B3LYP/6-31G(d)			PCM/BMK/6-31G(d)			λ_{exp}, nm
λ, nm	f	Assignment	λ, nm	f	Assignment	
C219						
732 (657)	1.045 (0.990)	91% HOMO → LUMO (88%)	571 (533)	1.838 (1.748)	73% HOMO → LUMO (74%)	493[a]
538 (503)	0.917 (0.896)	84% HOMO − 1 → LUMO (80%)	433 (411)	0.165 (0.152)	71% HOMO − 1 → LUMO (73%)	
451 (433)	0.228 (0.190)	84% HOMO → LUMO + 1 (78%)	377 (366)	0.316 (0.280)	76% HOMO → LUMO + 1 (77%)	387[a]
372 (365)	0.232 (0.198)	90% HOMO → LUMO + 2 (87%)	321 (316)	0.278 (0.284)	35% HOMO → LUMO + 2 (44%)	
306 (306)	0.288 (0.188)	81% HOMO → LUMO + 5 (87%)	275 (274)	0.294 (0.322)	51% HOMO → LUMO + 5 (71%)	
TPCADTS						
638 (569)	0.957 (0.933)	89% HOMO → LUMO (86%)	521 (482)	1.422 (1.347)	80% HOMO → LUMO (79%)	495[b]
456 (432)	0.651 (0.528)	81% HOMO − 1 → LUMO (78%)	386 (365)	0.173 (0.107)	78% HOMO − 1 → LUMO (79%)	336[b]
398 (379)	0.06 (0.05)	86% HOMO → LUMO + 1 (80%)	338 (327)	0.116 (0.09)	77% HOMO→LUMO+1 (77%)	
337 (335)	0.140 (0.270)	46% HOMO → LUMO + 2 (81%)	300 (297)	0.419 (0.397)	48% HOMO → LUMO + 2 (52%)	298[b]
309 (311)	0.112 (0.132)	65% HOMO → LUMO + 6 (67%)	278 (278)	0.271 (0.195)	76% HOMO → LUMO + 6 (73%)	

[a] Experimental data are taken from Ref. [1].
[b] Experimental data are taken from Ref. [2].

EDOT (DD for TPCADTS) spacers (Fig. 4). Note that this electronic transition is a productive process in the generation of electric current in the circuit. Relaxation of the excited state occurs by electron injection into the conduction band of the semiconductor. The efficiency of this process (IPEC) is more than 95% (80% for TPCADTS). Thus, the main efficiency losses are due to the recombination of electrons from the conduction band of a semiconductor with the redox pairs of the electrolyte (dark current). It gives a total efficiency of a solar cell at about 10–10.3% (6.65% for TPCADTS) under AM 1.5G condition using the highly volatile electrolyte [1,2].

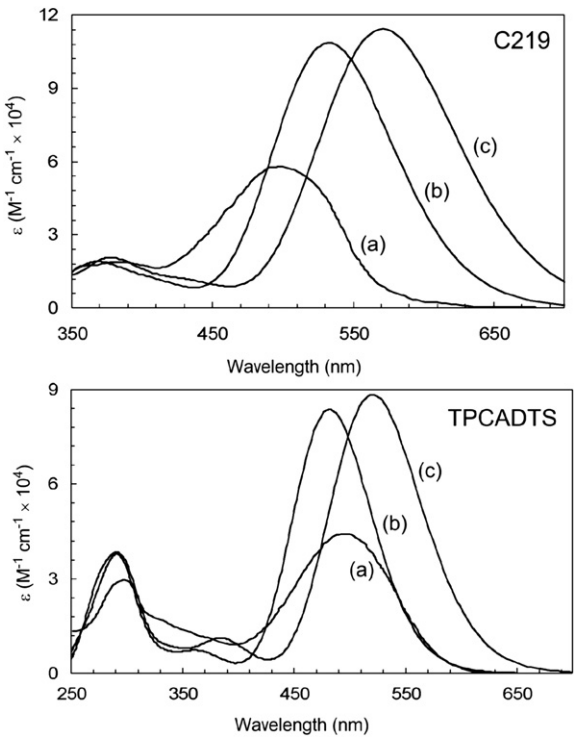

Fig. 3. Experimental (a) and theoretical spectra of C219 (top) and TPCADTS (bottom) dyes in gas phase (b) and with the PCM model (c). The experimental curves are taken from Refs. [1,2]. The theoretical curves were calculated by the BMK/6-31G(d) method.

An electron injection from the excited dye into the conduction band of the semiconductor occurs from the dye LUMO, which has a high density on the cyanoacrylic-acid acceptor group. By this group the dye is adsorbed on the TiO_2 semiconductor surface, thus the injection is induced by strong overlap between LUMO and the conduction band wave function. At the same time the ionized dye reduction by the electrolyte is determined mostly by the dye HOMO and its overlap with the redox pair orbitals of the electrolyte. Really, the reduction of the ionized dye (the cationic state of the dye) by the electrolyte involves the singly occupied molecular orbital (SOMO) of the dye cation [22], which is not necessarily the same function as the HOMO of the dye in the ground state. Our calculation of the C219 dye cation by spin-restricted B3LYP method indicates that the SOMO (Dye+) and HOMO (Dye) are very similarly shaped. We hope that the same analogy would be true for the TPCADTS dye, thus we can analyze and compare just the HOMOs of the dyes, presented in Fig. 4. In fact the HOMO of both dyes is localized not only on the triphenilamine donor group, but also on a big part of the linker (Fig. 4). In C219 this part is longer and provides better possibility for the dye–electrolyte interaction and electron transfer to the singly occupied HOMO of the excited dye. Thus its reduction by the redox pair of the electrolyte is more efficient.

The peak at 377 (386) nm is caused by a singlet–singlet π–π^* transition which corresponds to the HOMO → LUMO + 1 (HOMO − 1 → LUMO for TPCADTS) excitation. Short-wavelength band has a relatively low intensity but causes the absorption in the near UV range, which is present in the solar irradiation spectrum. In the experimental absorption spectrum of the TPCADTS dye is also observed the band peaked at 298 nm. According to calculated data, this band has a peak at 300 nm and corresponds to the HOMO → LUMO + 2 excitation.

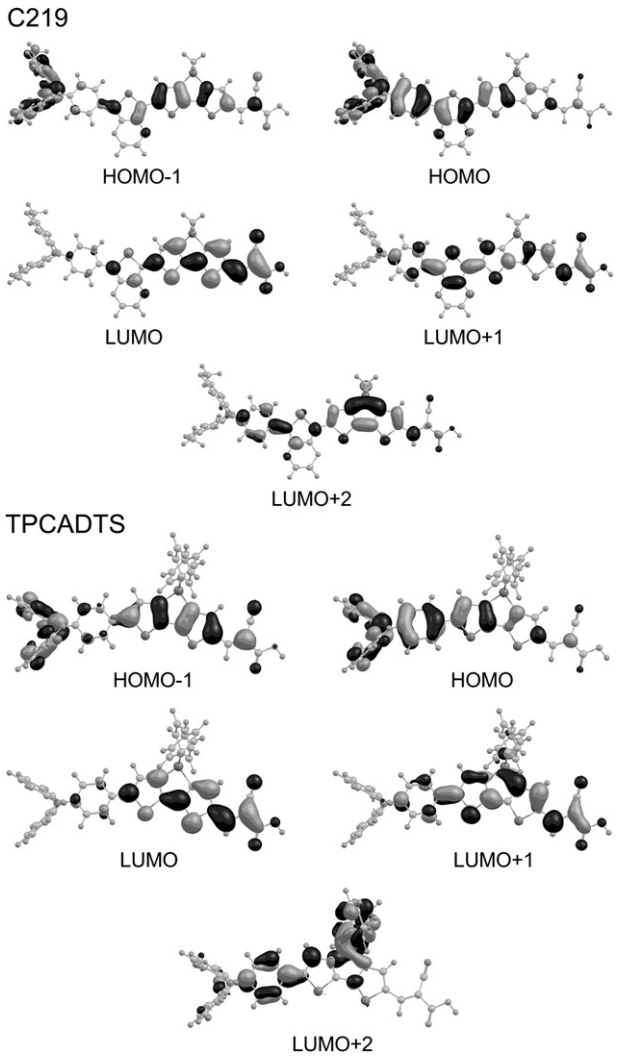

Fig. 4. Frontier molecular orbitals of C219 (top) and TPCADTS (bottom) dyes. Iso-density value 0.03 a.u.

As mentioned above the HOMO–LUMO excitation in C219 corresponds to electron transfer from triphenilamine to the cyanoacrylic-acid acceptor group through the EDOT and DHD conjugated spacer bridges (Fig. 4). At the same time the both orbitals have some nonzero electron density in the common molecular fragments: this concerns just the EDOT and DHD spacers. This is wrong to say that there is an overlap between two orbitals (as it is used to be sometimes [23]) since they are orthogonal being eigen-functions of self-consistent field method. Nonzero values of the HOMO and LUMO wave-functions in the same common part of molecular space is a very important property of the efficient dye-sensitizer for solar cell; it provides a large electric dipole transition moment for light absorption and also represents the main driving force for electron transfer from the dye to semiconductor. The C219 dye is adsorbed at the TiO_2 surface by the terminal deprotonated carboxy-group (right part at the top of Fig. 4). The HOMO–LUMO transition dipole moment vector is strongly oriented along the direction from donor to acceptor. Intermolecular interaction between the dye and the semiconductor can be expressed in terms of perturbation theory as a coupling of two transition dipole moments inside both particles [24]. Orientation of the vectors is also important. Transition moment between the ground and excited states inside the semiconductor can be considered as an entire property of the TiO_2 nanocrystal; it also can be enhanced (or induced) by the dye adsorption and interaction with the excited dye. Intermolecular dipole–dipole (or dipole-induced dipole) interaction has a pure quantum nature since we consider here quantum transition dipole moments, which are not observable values. (Only a square of this value enter the expression for the transition probability or intensity of light absorption [24]). Similar analysis can be applied for the TPCADTS dye and its analogs [2] (Fig. 4).

4. Conclusions

Triarylamine dyes with the dithienosilole π-conjugated spacer recently used in very efficient dye-sensitized solar cells [1,2] are studied by DFT approach and their absorption spectra are interpreted with the time-dependent DFT method. We explain a high intensity of the incident light absorption in the long-wavelength band of the dye and predict its polarization. Analysis of the transition dipole moment vector and HOMO–LUMO orbital nature allow us to understand the reason of the high incident photon-to-collected electron conversion efficiency and the driving force of electron injection to the semiconductor. The better performance of the C219 dye is explained by the longer bridge between the donor (D) and acceptor (A) moieties. The HOMO and LUMO being orthogonal orbitals, are mainly localized at the D and A parts; they do not overlap, but still have large contributions at the common atoms of the linker. This provides large transition dipole moment highly oriented on the long molecular axis and strong virtual dipole–dipole (dispersion) interaction between molecule and the semiconductor surface. Thus the length of the linker in the C219 dye correlates with electron injection rate and with efficiency of the dye–electrolyte interaction, which depends on HOMO delocalization through the bridge.

For the ground state equilibrium geometry we also analyze the electron density distribution function by the Bader method (QTAIM). In this way we explain the planarity of the studied dyes accounting the stabilizing intramolecular hydrogen bonds and Van der Waals interactions based on the characters of the Laplacian of the electron density in the critical points and the Cremer–Kraka energy density.

References

[1] Zeng W, Cao Y, Bai Y, Wang Y, Shi Y, Zhang M, et al. Efficient dye-sensitized solar cells with an organic photosensitizer featuring orderly conjugated ethylenedioxythiophene and dithienosilole blocks. Chem Mater 2010;22(5):1915–25.
[2] Lin L-Y, Tsai C-H, Wong K-T, Huang T-W, Hsieh L, Liu S-H, et al. Tsai A-I Organic dyes containing coplanar diphenyl-substituted dithienosilole core for efficient dye-sensitized solar cells. J Org Chem 2010;75(14):4778–85.
[3] O'Regan B, Grätzel M. A low-cost, high-efficiency solar cell based on dye-sensitized colloidal TiO_2 films. Nature 1991;353(6346):737–40.
[4] Ito S, Miura H, Uchida S, Takata M, Sumioka K, Liska P, et al. High-conversion-efficiency organic dye-sensitized solar cells with a novel indoline dye. Chem Commun 2008;41:5194–6.
[5] Becke AD. Density-functional thermochemistry. III. The role of exact exchange. J Chem Phys 1993;98(7):5648–52.
[6] Lee C, Yang W, Parr RG. Development of the Colle–Salvetti correlation-energy formula into a functional of the electron density. Phys Rev B 1988;37(2):785–9.
[7] Francl MM, Petro WJ, Hehre WJ, Binkley JS, Gordon MS, DeFrees DJ, et al. Self consistent molecular orbital methods. XXIII. A polarization type basis set for second row elements. J Chem Phys 1982;77(7):3654–66.
[8] Frisch M, Trucks G, Schlegel H, Scuseria G, Robb M, Cheeseman J, et al. Gaussian 03, revision C.02. Wallingford, CT: Gaussian, Inc.; 2004.
[9] Runge E, Gross EKU. Density-functional theory for time-dependent systems. Phys Rev Lett 1984;52(12):997–1000.
[10] Luo Y, Jonsson D, Norman P, Ruud K, Vahtras O, Minaev B, et al. Some resent developments of high-order response theory. Int J Quant Chem 1998;70(1):219–39.
[11] Boese AD, Martin JML. Development of density functionals for thermochemical kinetics. J. Chem Phys 2004;121(8):3405–16.

[12] Miertus S, Scrocco E, Tomasi J. Electrostatic interaction of a solute with a continuum. A direct utilization of *ab initio* molecular potentials for the prevision of solvent effects. Chem Phys 1981;55(1):117–29.
[13] Gorelsky SI. SWizard program. Ottawa, Canada: University of Ottawa, http://www.sg-chem.net/; 2010.
[14] Bader RFW. Atoms in molecules. A quantum theory. Oxford: Clarendon Press; 1990.
[15] Espinosa E, Molins E, Lecomte C. Hydrogen bond strengths revealed by topological analyses of experimentally observed electron densities. Chem Phys Lett 1998;285(3–4):170–3.
[16] Espinosa E, Alkorta I, Rozas I. About the evaluation of the local kinetic, potential and total energy densities in closed-shell interactions. Chem Phys Lett 2001;336(5–6):457–61.
[17] Cremer D, Kraka E. A description of the chemical bond in terms of local properties of electron density and energy. Croat Chem Acta 1984;57:1259–81.
[18] Bushmarinov IS, Lyssenko KA, Antipin MYu. Atomic energy in the "Atoms in molecules" theory and its use for solving chemical problems. Rus Chem Rev 2009;78(4):283–302.
[19] Nelyubina Yu V, Antipin MYu, Lyssenko KA. Anion–anion interactions: their nature, energy and role in crystal formation. Russ Chem Rev 2010;79(3):167–87.
[20] Keith TA. AIMAll (version 10.07.25), www.aim.tkgristmill.com; 2010.
[21] Baryshnikov GV, Minaev BF, Minaeva VA. Quantum-chemical study of structure and spectral properties of triphenilamine–rhodanine dye 2-(5-(4-(diphenylamine)benzylidene)-4-oxo-2-thioxothiazolidine-3-yl) acetic acid. Opt Spectrosc 2011;110(2):216–23.
[22] Nyhlen J, Boschloo G, Hagfeldt A, Kloo L, Privalov T. Regeneration of oxidized organic photo-sensitizers in Grätzel solar cells: quantum-chemical portrait of a general mechanism. Chemphyschem. 2010;11(9):1858–62.
[23] Köhler A, Bässler H. Triplet states in organic semiconductors. Mater Sci Eng R Rep 2009;66(4–6):71–109.
[24] Minaev BF. Quantum-chemical investigation of the mechanisms of the photosensitization, luminescence, and quenching of singlet $^1\Delta_g$ oxygen in solutions. J Appl Spectrosc 1985;42(5):766–72.